Preparation and Characterization of Maleic Anhydride-*g*-Polypropylene/Diamine-Modified Clay Nanocomposites

Moon Jo Chung,[1] Lee Wook Jang,[2] Jae Hun Shim,[2] Jin-San Yoon[2]

[1]*Howtech Corp., 430-1 Gasanri, Icheon-si, Gyeonggi-do 467-861, Korea*
[2]*Department of Polymer Science and Engineering, Inha University, Incheon 402-751, Korea*

Received 3 September 2003; accepted 29 March 2004
DOI 10.1002/app.21224
Published online in Wiley InterScience (www.interscience.wiley.com).

ABSTRACT: Polypropylene (PP)/montmorillonite (MMT) nanocomposites were prepared by compounding maleic anhydride-*g*-polypropylene (MAPP) with MMT modified with α,ω-diaminododecane. Structural characterization confirmed the formation of characteristic amide linkages and the intercalation of MAPP between the silicate layers. In particular, X-ray diffraction patterns of the modified clay and MAPP/MMT composites showed 001 basal spacing enlargement as much as 1.49 nm. Thermogravimetric analysis revealed that the thermal decomposition of the composite took place at a slightly higher temperature than that of MAPP. The heat of fusion of the MAPP phase decreased, indicating that the crystallization of MAPP was suppressed by the clay layers. PP/MAPP/MMT composites showed a 20–35% higher tensile modulus and tensile strength compared to those corresponding to PP/MAPP. However, the elongation at break decreased drastically, even when the content of MMT was as low as 1.25–5 wt %. The relatively short chain length and loop structure of MAPP bound to the clay layers made the penetration of MAPP molecules into the PP homopolymer phase implausible and is thought to be responsible for the decreased elongation at break. © 2004 Wiley Periodicals, Inc. J Appl Polym Sci 95: 307–311, 2005

Key words: nanocomposites; poly(propylene) (PP); organoclay

INTRODUCTION

Polypropylene (PP) exhibits an attractive combination of low cost, low weight, and extraordinary versatility in terms of properties, applications, and recycling.[1] To improve PP's competitiveness in engineering resin applications, it is an important objective to simultaneously increase its dimensional stability, stiffness, strength, and impact resistance. Therefore, a special emphasis has been placed on the development of nanofilled PP by means of inorganic or organic nanocomposites.

Recent studies on PP/clay nanocomposites have focused on the uniform dispersion of modified clay particles in the nonpolar matrix to maximize their physical and mechanical properties. Clay exfoliation has been pursued by the compounding of stearylammonium-exchanged montmorillonite (MMT), maleic anhydride-*g*-polypropylene (MAPP), and PP homopolymer with extrusion compounding.[2–7] Attempts to fully exfoliate clay particles in PP have been fraught with many challenges[8] because of the mismatch in surface polarities between clay and PP. The nanolayer exfoliation of PP remains much behind that of nylon/clay nanocomposites.

In this study, MAPP/MMT (PP/MMT) nanocomposites were prepared by simple amidation between the maleic anhydride group of MAPP and the amine groups of organomodified montmorillonite (OrMMT). The MAPP/MMT nanocomposites were compounded with PP. Characterizations of the structure, physical properties, and internal micromorphology of the nanocomposite materials were performed, and their results are discussed.

EXPERIMENTAL

Materials

The clay used for this study was Na^+ montmorillonite(NaMMT; Southeastern Clay Co., Gonzalez, TX). The cation exchange capacity of NaMMT was 92 mequiv/g. 1,12-Diaminododecane(DA; Aldrich) and titanium butoxide (Aldrich) were reagent grade and were used without further purification. The solvents were purified by two times of distillation.

Preparation of organophilic layered silicates

Typically, 30 g of NaMMT was dispersed in 1 L of deionized water. The temperature was raised to 80°C with gentle stirring. Then, 0.3 mol of DA and 0.1 mol of HCl were added to the mixture and stirred for 60 min. The precipitate was subjected to repeated inten-

Correspondence to: J.-S. Yoon (jsyoon@inha.ac.kr).
Contract grant sponsor: Inha University; contract grant number: INHA 30393.

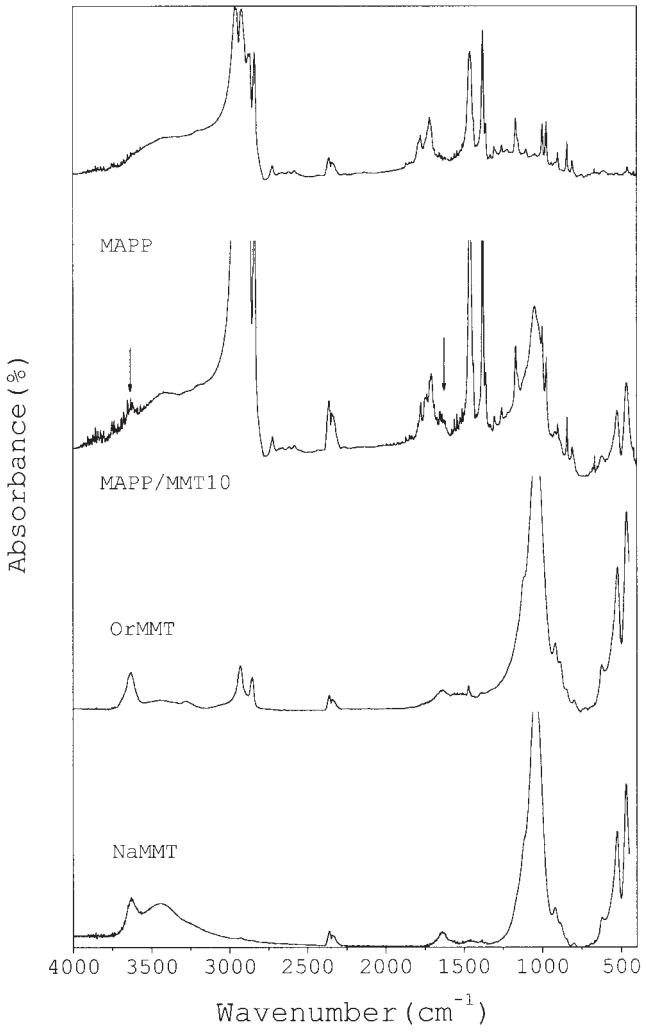

Figure 1 Fourier transform infrared spectra of NaMMT, OrMMT, MAPP, and an MAPP/MMT nanocomposite.

sive washing by four cycles of centrifugation and redispersion into water. The resulting silicates were dried under reduced pressure at 80°C for 1 week and were then ground to 10-μm particles in a ball mill.

Preparation of the MAPP/MMT nanocomposite master batch

A 500-mL reactor fitted with a thermometer and a condenser was charged with 300 mL of 1,2,4-trichlorobenzene followed by the addition of MAPP and the modified clay. The temperature was then raised to 160°C with gentle stirring. Titanium butoxide (10 μL) as a catalyst for the amidation reaction was introduced to the reactor. The reaction was terminated after 24 h by the quenching of the reaction mixture to room temperature.[9] The product was poured into a large amount of methanol. The precipitated products were separated and purified by several cycles of centrifugation and redispersion into methanol. The products were dried under reduced pressure at 80°C for 1 week.

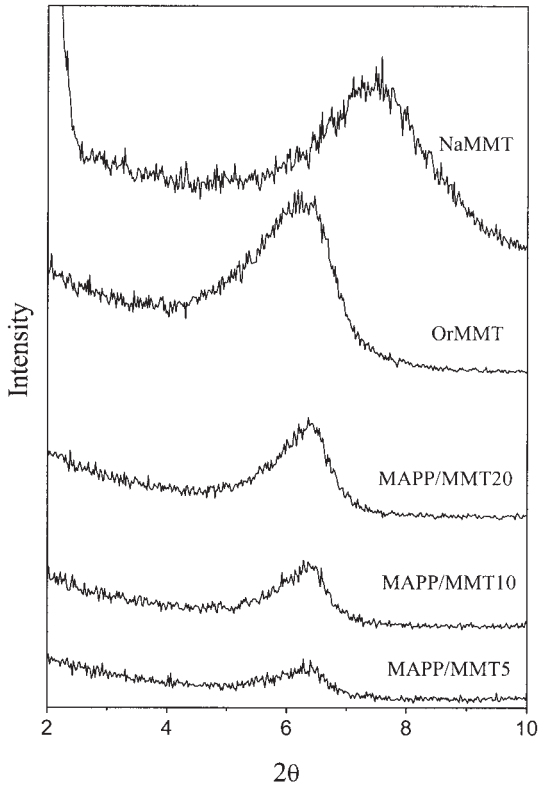

Figure 2 XRD patterns of NaMMT, OrMMT, and the MAPP/MMT nanocomposites.

Compounding of the MAPP/MMT master batch with PP

PP pellets and the MAPP/MMT nanocomposites master batch were melt-blended in Brabender mixer-(Plasti-Corder PLV151, Akron, OH) at 200°C and 50 rpm for 10 min. The obtained strands were pelletized. Sheets of 0.1 mm in thickness were made by melt pressing with a hot press (FREDS ARVER, Inc., model 2697, Wabashi, IN) at 200°C under 5 tons of pressure.

Polymer characterization

A Fourier transform infrared spectrum was recoded on a PerkinElmer Spectrum 2000 over a wave number

TABLE I
XRD Data of the OrMMT and MAPP/MMT Composites

Sample code	MAPP content in the composite	Interlayer distance	
		d (nm)	*d* (nm)[a]
NaMMT	—	1.18	—
OrMMT	—	1.40	0.22
MAPP/MMT 95/5	94.6	1.39	0.21
MAPP/MMT 90/10	90.6	1.39	0.21
MAPP/MMT 80/20	83.2	1.39	0.21

[a] Increase in the interlayer distance of the montmorillonite induced by loading of the organics.

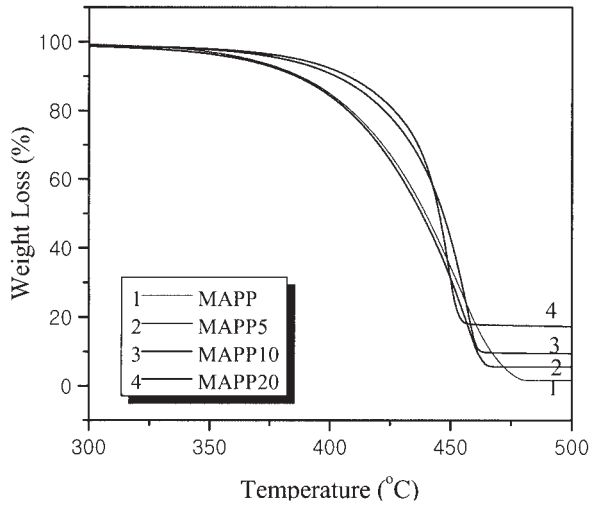

Figure 3 TGA thermograms of MAPP and the MAPP/MMT nanocomposites.

range of 4000–400 cm^{-1}. The variation of the interlayer distance of MMT in the nanocomposites was studied by means of wide-angle X-ray scattering with a Rigaku DMAX 2500 (Danvers, MA). The Cu Kα radiation source was operated at 40 kV and 40 mA. We recorded patterns by monitoring those diffractions appearing in the 2θ range from 2 to 10° with a scanning rate of 1°/min. The average molecular mass and polydispersity of the products were measured by size exclusion chromatography equipped with a Waters 510 pump (Boston, MA), refractive index (RI) and ultraviolet detectors, a Rheodyne injector, and four linear columns packed with μ-Styragel. The flow rate of THF was 1.0 mL/mm, and the columns were calibrated with polystyrene standards. We carried out the thermogravimetric analysis (TGA) of the products by heating the samples to 600°C at a heating rate of 20°C/min under a nitrogen atmosphere with a TA Instrument thermogravimetric analyzer (New Castle, DE). Thermal behavior was analyzed by differential scanning calorimetry (DSC; PerkinElmer DSC 7). The sample was heated to 200°C at a heating rate of 20°C/min under a nitrogen atmosphere(first scan) and then cooled to 30°C at −100°C/min to observe the crystallization peak. The sample was reheated to 200°C at 20°C/min (second scan), and the second scan thermogram was used as data. The tensile properties of the composites were measured with a universal testing machine (Hounsfield Co., H 10KS-0061, Horsham, PA). Specimens were prepared according to ASTM D 638. The crosshead speed was 60 mm/min. The results from five specimens were averaged. The morphological aspects of the composites were examined with transmission electron microscopy (TEM) to determine their internal micromorphologies. A Jeol-200 CX transmission electron microscope (Peabody, MA) with an acceleration voltage of 200 kV was used. The state of MMT dispersion in the composites was examined through optical microscopy (OPTIPHOT2-POL Polarizing microscope, Nikon, Tokyo, Japan).

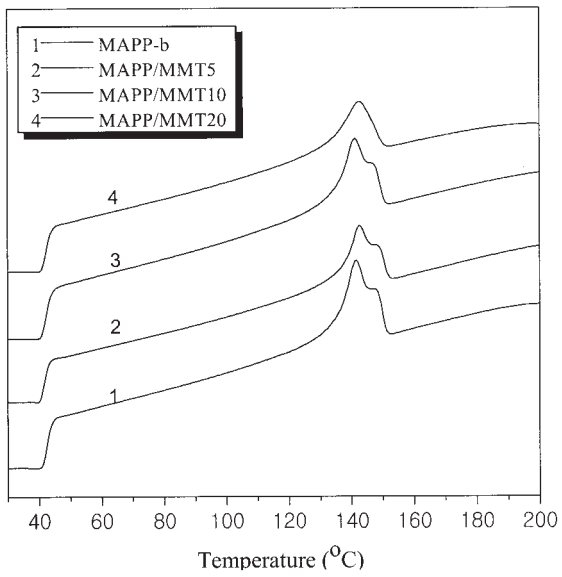

Figure 4 DSC thermograms of MAPP and the MAPP/MMT nanocomposites.

RESULTS AND DISCUSSION

Structural characterization

The MAPP/MMT nanocomposites were prepared by a simple amidation reaction between the maleic anhydride group of MAPP and the amine groups of the OrMMT. Figure 1 compares the IR spectra of the composites with those of pristine MAPP and MMT. Evidently, the composites exhibited characteristic absorptions because of the organic and inorganic functional groups. The absorptions at 3630 and 1050 cm^{-1} were associated with —OH stretching of the lattice water and Si—0 stretching of MMT, respectively. The absorption band appearing at 1750 cm^{-1} (C═O stretching) was due to the MAPP moiety. The absorption at 1650 cm^{-1} was attributed to primary amide C═O stretching, which confirmed that the amidation reaction took place during the compounding. This spectral

TABLE II
Thermal Properties of Neat MAPP and the MAPP/MMT Nanocomposites

Sample code	T_m	ΔH_f
MAPP[a]	141.6	72.8
MAPP/MMT5	142.7	62.5
MAPP/MMT10	142.2	56.5
MAPP/MMT20	142.5	48.3

[a] MAPP processed at the same conditions as for the preparation of the MAPP/MMT composites.

TABLE III
Mechanical Properties of the PP Homopolymer Compounded with MAPP/MMT

Sample code	Yield strength (MPa)	Tensile modulus (MPa)	Yield strain (%)
PP/MAPP[a]	12.6 ± 1.2	470 ± 5	40.2 ± 4.5
PP/MAPP/MMT5[b]	15.2 ± 1.0	640 ± 3	5.6 ± 0.5
PP/MAPP/MMT10[c]	15.7 ± 1.5	590 ± 9	5.2 ± 0.6
PP/MAPP/MMT20[d]	15.9 ± 1.9	568 ± 11	5.2 ± 0.9

[a] PP (75 wt%) compounded with MAPP (25 wt%).
[b] PP (75 wt%) compounded with MAPP/MMT5 (25 wt%).
[c] PP (75 wt%) compounded with MAPP/MMT10 (25 wt%).
[d] PP (75 wt%) compounded with MAPP/MMT20 (25 wt%).

analysis offered qualitative evidence of MAPP intercalation in the layers of MMT.

Figure 2 shows the X-ray diffraction (XRD) patterns of the MAPP/MMT composites, OrMMT, and NaMMT. Undoubtedly, the overall patterns of the composites were essentially the same as those of the pristine NaMMT, except for the peak corresponding to 001 reflection. This proved that the overwhelming fraction of the composite retained the crystalline structure of NaMMT. The interlamellar distance calculated from the position of 001 reflection is listed in Table I along with the data for the polymer content in the composite determined from the weight loss during TGA, as demonstrated in Figure 3. The peak position of pristine NaMMT at $2\theta = 7.4°$ (1.17 nm) shifted to a smaller angle of $2\theta = 6.2°$ (1.40 nm) when the NaMMT was modified by DA.

When MAPP was compounded with OrMMT, however, the d-spacing was not enlarged any further. The interlayer distance of MAPP/MMT (1.39 nm) compared with that of NaMMT (1.17 nm) provided an estimation of the chain conformation of the intercalated polymer molecules; that is, the polymer chains ran parallel to the interlayer with extended conformation. Accordingly, the MAPP molecules could be in-

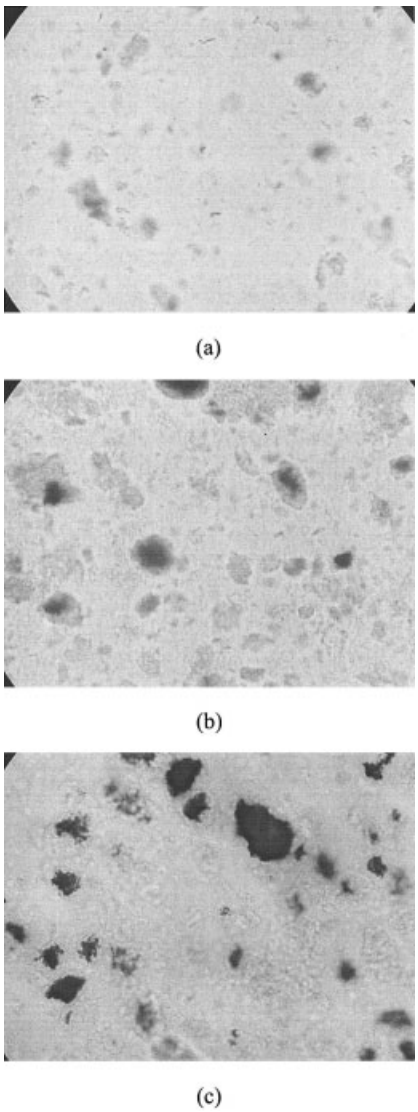

Figure 5 Optical micrographs of the nanocomposites: (a) MAPP/MMT5, (b) MAPP/MMT10, and (c) MAPP/MMT20.

Figure 6 Micrograph of the MAPP/MMT5 nanocomposite.

tercalated into the interlayer of MMT without a significant delamination of the clay layers. Therefore, the decreased interlayer distance of OrMMT after compounding with MAPP did not exclude the possibility of a reaction between OrMMT and MAPP. The amidation reaction between MAPP and the amine groups of OrMMT may have stretched molecules and, thereby, somewhat decreased the interlayer distance of OrMMT.

Thermal characterization

The onset temperature of weight decrease in TGA moved to a higher temperature region as the content of OrMMT in the composite increased. On the basis of the fact that inorganic species have good thermal stabilities, it is generally believed that the introduction of inorganic components into organic materials can improve their thermal stability. This increase in thermal stability could be attributed to the high thermal stability of clay and to the interaction between the clay particles and the polymer matrix, indicating that MAPP/MMT did not exist as a simple mixture. It confirmed that a chemical reaction between MAPP and MMT should have occurred.

The thermal properties, as measured by DSC, of the polymers shown in Figure 4 are collected in Table II. The peak melting temperature (T_m) and the heat of fusion (ΔH_f) were observed while the cooled sample was reheated from 30°C at 20°C/min. ΔH_f of the composites decreased as the MMT content increased. This occurred because MMT firmly seized the chemically bound MAPP molecules, making crystallization more difficult.

Mechanical characterization

Table III shows the mechanical properties of the composites. Specimens of the MAPP/MMT composites for the test of the mechanical properties could not be prepared because of their powdery texture; MAPP/MMT composites were blended with the PP homopolymer, and specimens were prepared for the tensile tests. The weight ratio of MAPP/MMT and the PP homopolymer was fixed at 25:75. The ultimate strengths of the composites increased by 25% from 12.6 to 15.9 MPa. The tensile modulus also increased from 470 to 570–640 MPa because of resistance exerted by the clay layer against plastic deformation. Additionally, the stretching resistance of the oriented backbone chains in the gallery should have also contributed to the enhancement of the modulus.[9–11] However, the elongation at break decreased drastically, even when the content of MMT was as low as 1.25–5 wt %.

MAPP molecules bound to OrMMT should have had loop conformations because the several anhydride units of MAPP could have reacted with the amine groups of OrMMT at the same time. The relatively low weight-average molecular weight of MAPP made chain entanglements of MAPP with PP practically implausible. MAPP molecules with loop conformations should have much longer chain length than linear MAPP ones so as to chain entangle with PP. Therefore, MAPP bound to OrMMT particles could hardly penetrate into the PP homopolymer phase but rather existed as a discretely dispersed phase in the blend to form weak points where the initiation of the failure took place during the tensile tests. This effect was thought to be responsible for the decreased elongation at break. Further research is required to compound OrMMT with high-molecular-weight MAPP. For this purpose, a special scheme of synthesis should be devised because grafting maleic anhydride on PP is usually accompanied by the chain scission of PP molecules.

Morphology of the composite

Figure 5 shows the optical micrographs of the composites. The micrographs exhibit well the dispersed morphological aspect of the composites. However, the aggregation of MMT particles appeared as the MMT content increased. Wide-angle X-ray diffraction is a conventional method for determining the interlayer spacing of clay layers in the original clay and in the intercalated polymer/clay nanocomposites. However, the internal structure of the nanocomposites on a nanometer scale could be examined by observation through TEM. TEM allows a qualitative understanding of the internal structure through direct observation. Typical TEM photographs for the composites are displayed in Figure 6. The dark lines in the pictures represent clay layers 1 nm thick. The gap between the dark lines corresponds to interlayer spaces, and the MAPP matrix is shown by the gray background. It was clearly observed from the TEM image that 1–2-nm silicate layers were arranged in good order and were well dispersed in the polymer matrix.

References

1. Moore, E. P. Polypropylene Handbook; Hanser: Munich, 1996.
2. Nam, P. H.; Maiti, P.; Okamoto, M.; Kotaka, T.; Hasegawa, N.; Usuki, A. Polymer 2001, 42, 9633.
3. Kawasumi, M.; Hasegawa, N.; Kato, M.; Usuki, A.; Okada, A. Macromolecules 1997, 30, 6333.
4. Hasegawa, N.; Okamoto, H.; Kawasumi, M.; Kato, M.; Tsukigase, A.; Usuki, A. Macromol Mater Eng 2000, 280/281, 76.
5. Hasegawa, N.; Okamoto, H.; Kato, M.; Usuki, A. J Appl Polym Sci 2000, 78, 1918.
6. Lan, T.; Qian, G. Q. In Proceedings of Additives '00, Clearwater Beach, FL, Apr 2000.
7. Dennis, H. R.; Hunter, D. L.; Chang, D.; Kim, S.; White, J. L.; Cho, J. W.; Paul, D. R. Polymer 2001, 42, 9513.
8. Manias, E.; Touny, A.; Wu, L.; Strawhecker, K.; Lu, B.; Chung, T. C. Chem Mater 2001, 13, 3516.
9. Lee, D. C.; Jang, L. W. J Appl Polym Sci 1996, 61, 1117.
10. Lee, D. C.; Jang, L. W. J Appl Polym Sci 1998, 68, 1997.
11. Jang, L. W.; Kang, C. M.; Lee, D. C. J Polym Sci Part B: Polym Phys 2001, 39, 719.